IMPROVEMENT OF CHARACTERISTICS OF AISI 310 GRADE STAINLESS STEEL MATERIAL BY CARBURIZING

Manne Vamshi[1,*], *J.* Saranya[2], *Ram* Subbiah[2]

[1] PG Student, Gokaraju Rangaraju Institute of Engineering and Technology, Hyderabad, India
[2] Associate Professor, Mechanical Engineering Gokaraju Rangaraju Institute of Engineering and Technology, Hyderabad, India

Abstract. The investigation on the microstructure and mechanical behaviour of steel AISI 310 has been carried out during a Carburizing process aiming to improve the wear performance. The comparision study was made to treated specimens with untreated sample. Carburizing is a viable technique to enhance the wear resistance of the stainless steel material. The present study focused in the direction of investigating the effect of microstructure, hardness and wear resistance of AISI 310 stainless steel material. In carburizing process the case depth is found to be 11.5, 12, 14 Microns which is treated 2 hrs, 4hrs and 6 hrs respectively. The combination action of strong adhesion, abrasion and severe plastic deformation are the primary reasons for the continuous material loss in the untreated specimens during testing. The Optical microscope, SEM analysis and wear test are conducted to find out the various results

1 Introduction

Stainless steels might be grouped by the crystal structure of their matrix which can be martensitic, austenitic and ferritic and duplex (blend of ferritic and austenitic steel) stainless steels. Carburizing is a heat treatment process that diffuses carbon on surface of a metal to make a hardened surface. These processes are most normally utilized on low-carbon, low-alloy steels.

In the event that a material is exposed to gases containing carbon, for example as CO, CO2 or CH4 it can get carbon. The level of carburization is governed by the degree of carbon and oxygen in the gas, the temperature and the steel composition. The carbon which is attained by the steel will to a great extent from carbides. Carbon gets causes embrittlement of stainless steel because of carbides development, or even a system of carbides, in the grain limits just as inside the grains. The protection from thermal cycling is diminished and since carburization prompts an expansion in volume and there is a risk of cracks in the material. When ferritic steels are heated to temperatures over 950 ◦C, they endure precipitation of carbides during the ensuing cooling, and this causes a decrease in toughness and corrosion resistance. The precipitates framed in the grain boundaries cause intergranular corrosion and in extraordinary cases, even decreases in toughness. The ferrite–pearlite steels, utilized in components of equipments before service have a BCC Fe (or ferrite) Structure with pearlite (or bainite) framing bars of ferrite and Fe carbides (Fe3C) [1]. After assistance the microstructure presents changes. The carbides change from bars to circles influencing the mechanical properties of steels on the grounds that the spheroid carbides debilitate the structure and help the dislocation movement by decreasing the intergranular anchorage [2]. A few authors have named the carbides as M3C, M6C and M23C6 where M is mixture of metallic molecules [4]. The formation of a protective surface oxide film gives beginning protection against metal defilement, yet the local rupture of surface oxide films permits fast carbon dispersion into the alloys [5].

As indicated by the current outcomes, the steels with high chromium and nickel content shows better corrosion resistance in the high temperature S−CO2 condition while the less alloyed steels perform ineffectively [6,7]. It is commonly acknowledged that high chromium substance can successfully improve the corrosion resistance of SSs due to the arrangement of continuous protective film. Then again, nickel is an alloying component most normally utilized as austenite stabilizer, and imparting nickel content in steels prompts the change of ferrite/martensite to austenite. Up to now, the impact of matrix structure (fundamentally tuned by nickel content) of SSs on the corrosion behaviour in the S−CO2 condition is as yet not extremely clear, in light of the fact that the nickel and chromium substance change at the same time in numerous commercial SSs [8].

* Corresponding author: vamshimanne96@gmail.com

Ferritic hardened steels are contender for applications in the high temperature parts of the cycle due to their great heat transfer properties and mechanical properties yet their protection from environmental degradation [9]. As of late, studies prompted by the uprising enthusiasm on S-CO2 cycle for power plants wound up to new papers on the corrosion behaviour of 9-12Cr ferritic–martensitic steels in CO2 at temperatures up to 650◦C and 250 bar [10–14]. Also, results on the corrosion behaviour of 9-12Cr steels in CO2 at temperatures between550◦C and 700◦C have been displayed in the literature for a few years in the framework of candidate materials for oxy-fuel ignition process in coal-power plants [15–17]. From an arrangement of these examinations, it very well may be inferred that a large portion of the 9-12Crsteels oxidize and carburize in CO2 at temperatures higher than 500◦C. Their oxidation rate is multiple sets of greatness quicker than normal 18Cr austenitic steels. They structure a "protective" duplex oxide scale made of an external magnetite/haematite layer with coarse columnar grains and a nearly as-thick internal Fe–Cr rich spinal oxide layer made of little equiaxed grains. Underneath the scale, Cr rich carbides structure and their density and penetration depth increase with time.

Carbon dioxide turns into a supercritical liquid when temperature and pressure exceed the critical point of CO2 (31.26 C, 72.9 atm). Until now, there are a few examinations about the corrosion behaviour of candidate structural materials in high temperature and pressure S-CO2 condition. Along these lines, it is important to adequately assess high-temperature corrosion of materials on the grounds that unreasonable corrosion may threaten the basic structural integrity and disintegrate the heat transfer capacity.

Corrosion conduct of a few candidate materials in high temperature CO2 has been widely considered. Rouillard et al. [19] have explored the high-temperature corrosion behaviour of 9Cr and 12Cr ferritic-martensitic (F-M) steel under CO2, pressures varying from 1 to 250 bar for exposure of 8000 h. The outcomes indicated that the oxidation rate was not really influenced by the expanding CO2 pressure however expanded the carburization rate. Tan et al. [20] detailed the erosion conduct of F-M steels presented to S-CO2 at 650oC and 20.7 MPa. The F-M steels indicated poor oxidation resistance and thick oxide scales spallation happened effectively. Propp et al. [21] researched the corrosion of ferritic steels and austenitic stainless steels in S- CO2 in the temperature scope of 150-240oC and pressure variation of 8.7-15.7 MPa. They found that the corrosion rate in carbon steels is up to multiple times higher than austenitic stainless steels.

Table 1.1 Composition of AISI 310 ASS

Elements	C	Mn	Si	P	S	Cr	Mo	Ni
%	0.25	2.0	1.5	0.045	0.03	26	2.00-3.00	22

2 Experimental procedure

The pin type AISI 310 grade stainless steel were reduce into small pieces of size 30mm, diameter 8 mm, with the assist of wire cut EDM process and disc of equal fabric is used, with 150mm diameter and 10 mm thickness. The disc fabric used to be floor hardened. Material composition: Carbon: 0.25%, manganese: 2.0%, silicon: 1.5%, sulphur: 0.03%, phosphorous: 0.045%, nickel: 22%, chromium: 26%. Mechanical specification: Tensile strength: 520 mpa, yield strength: 205 mpa, elongation: 40 %. Carburizing was done for the three specimens for CB11 – 2hr, CB22 – 4hr, CB33 – 6hr. Procedure of wear test with the pin was held against the counter face of a rotating disc. The pin was loaded against the disc through a dead weight loading system. The wear test for all specimens was conducted under the normal loads of 30N and 40Nrespectively. The wear rate was calculated from the height loss technique and expressed in terms of wear volume loss per unit sliding distance [18]. In this, the test was conducted with the parameters like Load, Speed and Distance. In the present experiment the parameters such as speed, time and load are kept constant throughout for all the experiments.

Table 2.1 Wear test working parameters

Parameter	**Value**
Load	30N,40N
Constant Track diameter	10mm
Diameter of disc	150mm
Height of disc	10mm
Diameter of pin	8mm
Length of pin	30mm
Material of disc	Stainless steel
Material of pin	310
Speed	500 rpm
Density	8000kg/m³
Time	5 mins(constant)

Table 2.2 – Wear track reading at 30N load

SNO	SPECIMEN	weight before testing (gms)	weight after testing(gms)	weight loss (gms)	volume wearloss (mm^3)	frictional force(n)
1	UNT	11.64	11.568	0.072	9	5.7
2	CB1	11.75	11.726	0.024	3	8.2
3	CB2	11.63	11.612	0.018	2.25	10.9
4	CB3	12.09	12.077	0.013	1.625	18.6
5	CN1	9.66	9.645	0.015	1.875	12.0
6	CN2	11.91	11.902	0.008	1	15.2
7	CN3	11.97	11.966	0.004	0.5	20.2

Table 2.3 – Wear track reading at 40N load

SNO	SPECIMEN	Weight before testing (gms)	Weight after testing (gms)	Weight loss (gms)	Volume Wear loss (mm^3)	Frictional Force(N)
1	UNT	11.568	11.470	0.098	12.25	3.6
2	CB11	9.06	8.998	0.062	7.75	5.0
3	CB22	8.64	8.600	0.040	5.0	8.9
4	CB33	8.37	8.358	0.012	1.5	9.5
5	CN11	8,82	8.76	0.060	7.5	1.63
6	CN22	7.90	7.857	0.043	5.3	3.6
7	CN33	8.49	8.456	0.034	4.25	10.5

3 Result and Discussion

The thickness of the nitrided specimens was measured under the Optical Microscope. The type of Optical Microscope used is of Olympus GX51 version with a magnification range of 5X - 100X .To find the coating thickness of the specimens; they were first cut into a small 3mm disc and are mounted into a disc by cold setting process. The process of setting involves placing the cut specimen into a mounting disc and adding silica or Bakelite powder and setting liquid and leaving them aside for 30 min to fuse together around under the chemical reaction. This mounting is removed from the cold setting disc and made to rub against various grades of emery paper starting from grit size 160 to 1200 until a smooth mirror faced finish is obtained. This mounted specimen is made to observe at various magnifications and at the range of 100X a clear view of coating thickness is obtained. The coating thickness is measured from the measurement table on horizontal/vertical distance between the two selected points i.e. one on the specimen edge and the other on the coating thickness edge.

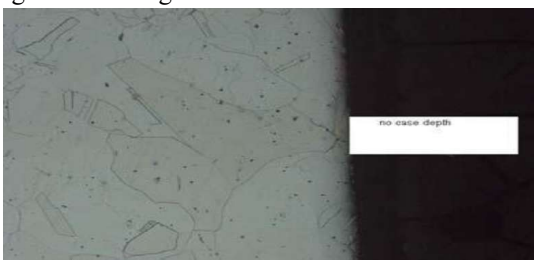

Fig. 3.1 Optical Microscope results for untreated specimen

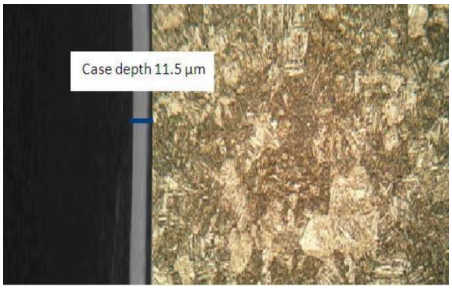

(1)

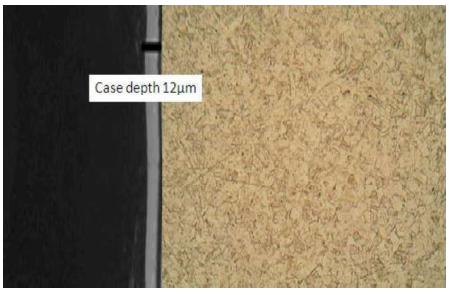

(2)

(3)

Fig. 3.2 Optical microscopy images of Carburizing specimen CB11, CB22 and CB33.

As the specimen CB11 is heat treated for 2hrs the specimen case depth is 11.5µm. As the specimen CB22 is heat treated for 4hrs the specimen case depth is 12µm. As the specimen CB3 is heat treated for 6hrs the specimen case depth is 14µm. Surface morphology and microstructural analysis of 310 Austenitic stainless steel is carried out before and after surface treatment under scanning electron microscopy (SEM) using SEM-JEOL-JSM- 6480 LV machine operated at an acceleration voltage of 15 kV. SEM makes use of the focused beam of the high-energy electrons to generate a variety of signals at the surface of solid specimens. The signals obtained from the electron beam and surface interaction gives the information about its morphology or texture. Generally the beam is focused onto a specified area of the specimen. The analysis of the samples was done at 5000x.

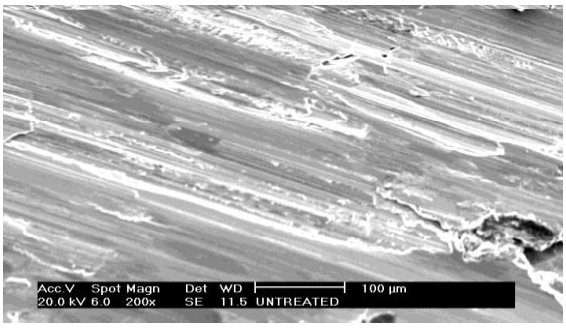

Fig 3.4 SEM image of untreated specimen

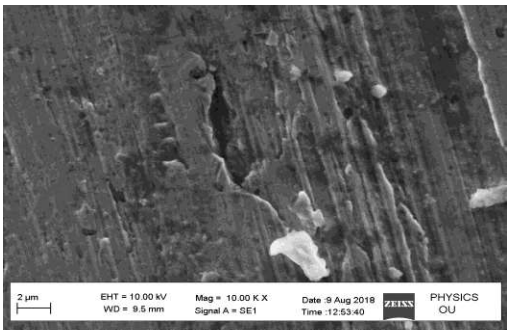

(1)

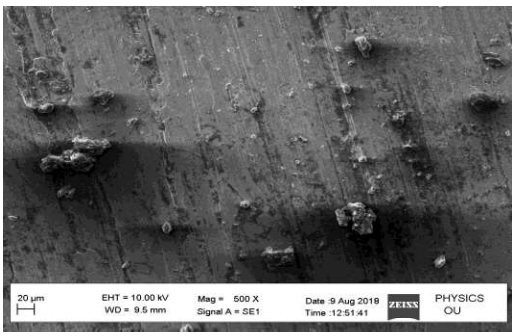

(2)

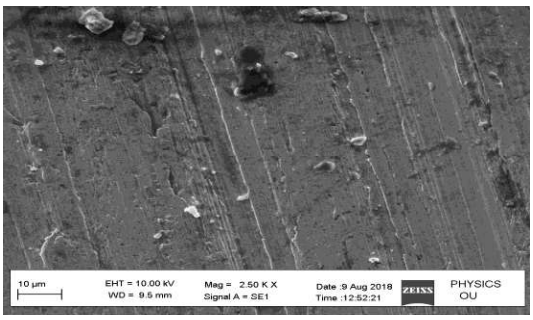

(3)

Fig. 3.5 SEM images of Carburizing specimen CB11, CB22 and CB33.

From the scanning electron microscope results, it was found that more peel of material from untreated specimen. As the time of heat treatment increases, wear decreases and wear loss decreases on the stainless steel material. There found to be less wear of material when it is subjected to load. Thereby wear resistance of the material increases, improving the property of ductility in stainless steel material and thereby increasing the hardness

4 Conclusion

In this work carburizing treated 310 grade stainless steels was performed and the wear behaviour was studied. Here a comparison study was made to treated specimens with untreated sample. Carburizing is a viable technique to enhance the wear resistance of the stainless steel material. Several researchers investigated the effect of carburizing on mechanical and surface behaviour of carbon steels. Only little information is available on the wear behaviour of AISI 310 grade austenitic stainless steel material. The present study focused in the direction of investigating the effect of microstructure, hardness and wear resistance of AISI 310 stainless steel material. The major conclusions are as follows.

1. In carburizing process the case depth is found to be 11.5, 12, 14 Microns which is treated 2 hrs, 4hrs and 6 hrs respectively.
2. From the pin on disc- wear study it was found to be that, CB specimen has a very highest wear resistance to time. The wear loss in carburizing process (CB1, CB2, CB3) were found to be 3.00, 2.25, 1.625 mm^3 at 30 N, 7.75, 5.0, 1.5 mm^3 at 40 N.
3. The combination action of strong adhesion, abrasion and severe plastic deformation are the primary reasons

for the continuous material loss in the untreated specimens during testing. Whereas the wear on the carburizing specimen due to less case depth wear is reduced.

4. As the time for treatment increases the case depth, hardness increases. In general, the wear resistance of the carburizing specimens is found to be superior to the untreated specimens.

References

1. S. Simonettia,b, C. Lanzc, G. Brizuelaa Juana, Materials Science and Engineering A **527** (2010)
2. J.D.Parker, Proceeding of Ninth International Symposium, 1996, p. **122**.
3. J.H. Woodhead, A.G. Quarrell, J. Iron Steel Inst. **203** (1965) 605.
4. L Toft, L. Marsden, Iron Steel Inst. 70 (1961) **276**.
5. C. Chun, G. Bhargava, T. Ramanarayanan, J. Electrochem. Soc. (2007) **154**.
6. H.J. Lee, S.H. Kim, H. Kim, C. Jang, Appl. Surf. Sci. **388** (2016).
7. Suresh Kumar T, Sankar V, *2011 IEEE India Conference, INDICON,* 2011
8. Hongsheng Chena,b, Sung Hwan Kima, Chaewon Kima, Junjie Chena, Changheui Janga,∗ Corrosion Science **156** (2019)
9. F. Rouillarda, T. Furukawab. Corrosion Science xxx (2016) xxx–xxx
10. L. Tan, M. Anderson, D. Taylor, T.R. Allen, Corros. Sci.**53** (2011).
11. F. Rouillard, F. Charton, G. Moine, Corrosion **67**(2011).
12. T. Furukawa, Y. Inagaki, M. Aritomi, Prog. Nucl. Energy **53** (2011).
13. F. Rouillard, G. Moine, L. Martinelli, J. Ruiz, Oxid. Met **77** (2012).
14. T. Furukawa, F. Rouillard, Prog. Nucl. Energy **82** (2014).
15. G.H. Meier, K. Jung, N. Mu, N.M. Yanar, F.S. Pettit, J.P. Abellan, T. Olszewski, L.N. Hierro, W.J. Quadakkers, G.R. Holcomb, Oxid. Met. **74** (2010).
16. T. Gheno, D. Monceau, J.Q. Zhang, D.J. Young, Corros. Sci. **53** (2011).
17. Tummala Suresh Kumar, Kosaraju Satyanarayana, Materials Today: Proceeding, 26 (2), 2020.
18. Manikonda, R. D., Kosaraju, S., Raj, K. A., & Sateesh, N., Material Today 5, 20104-20109. (2018).
19. Tan L, Anderson M, Taylor D, et.al. Corros Sci 2011;**53**.
20. Propp WA, Carleson TE, Wai CM, et al. Lockheed Idaho Technologies Co. Idaho Falls; 1996.